IETE Journal of Research
Publication details, including instructions for authors and subscription information:
http://www.tandfonline.com/loi/tijr20

Design and Simulation of a Zinc Oxide Thin Film Bulk Acoustic Resonator Filter for 2.6 GHz Band Applications

Jyotirmoy Dutta[a], Atul Vir Singh[a], Sonal Singhal[a] & Madhur Deo Upadhayay[a]
[a] Department of Electrical Engineering, School of Engineering, Shiv Nadar University, Greater Noida, UP, India
Published online: 24 Jul 2015.

IETE JOURNAL OF RESEARCH, 2015
http://dx.doi.org/10.1080/03772063.2015.1062734

Design and Simulation of a Zinc Oxide Thin Film Bulk Acoustic Resonator Filter for 2.6 GHz Band Applications

Jyotirmoy Dutta, Atul Vir Singh, Sonal Singhal and Madhur Deo Upadhayay

Department of Electrical Engineering, School of Engineering, Shiv Nadar University, Greater Noida, UP, India

ABSTRACT
This work presents the design and simulation of a zinc oxide based thin film bulk acoustic resonator (TFBAR) bandpass filter for 2.6 GHz band applications. Third and fifth-order filters in ladder topology are designed and compared. The third-order filter has an insertion loss of 1.62 dB and return loss of 18.97 dB with a bandwidth of 80 MHz whereas the fifth-order filter has insertion loss, return loss, and bandwidth of 2.85 dB, 25.28 dB, and 60 MHz, respectively. With a central frequency of 2.67 GHz, the designed filter has applications in the 2.6 GHz (2500−2690 MHz) band, which has been identified by the International Telecommunication Union as a global frequency band for mobile broadband services.

KEYWORDS
Bandpass filter; MBVD equivalent; TFBAR; 2.6 GHz band

1. INTRODUCTION

Most communication systems are now operating in the 1−5 GHz frequency range as the band below 1 GHz is almost fully occupied [1]. Radio frequency (RF) filters are one of the most important components of these systems. Although the surface acoustic wave filters have been in use for a long time, they are limited to 2 GHz operating frequency and have drawbacks like sub-micron lithography, expensive non-silicon substrates such as $LiNbO_3$ or $LiTaO_3$, and poor power handling capabilities [2]. Bulk acoustic wave (BAW) filters, on the other hand, operate at higher frequencies, have low losses, small size, and being bulk devices, have better power handling capabilities. They can be fabricated through standard IC technology processes and can be directly integrated with RF active circuits [3−5]. They can also be made tunable to work at different frequency bands [6−11].

One of the variants of the BAW resonator is the thin film bulk acoustic resonator (TFBAR). It consists of a thin-film piezoelectric material sandwiched between two metal electrodes as shown in Figure 1. When an alternating voltage is applied to the two electrodes, the piezoelectric layer expands and contracts giving rise to an acoustic wave. This wave travels vertically through the bulk of the material. A resonance condition occurs when the thickness of the piezoelectric layer is an integer multiple of half of the wavelength. The resonant frequency is given by

$$f_N = \frac{\vartheta N}{2t} \tag{1}$$

where ϑ is the longitudinal acoustic velocity, N is an integer, and t is the thickness of the piezoelectric layer [12,13]. The TFBAR device has two resonance frequencies, series resonance frequency (f_s), when polarization is in phase with the applied electric potential and a parallel resonance (anti-resonance frequency) frequency (f_p), when polarization is 180° out of phase with the applied electric potential [5]. The difference between f_s and f_p determines the electromechanical coupling coefficient, K^2_{eff}, of the TFBAR, a parameter that defines the bandwidth of the filter required for a particular application [12]. The expression for K^2_{eff} is as below [12]:

$$K^2_{\mathrm{eff}} = \frac{\pi^2}{4} \cdot \left(\frac{f_s}{f_p}\right) \cdot \left(\frac{f_p - f_s}{f_p}\right) \tag{2}$$

A bandpass response could be obtained by arranging TFBARs with slightly shifted frequency response in a ladder topology, lattice topology, or a combination of both. The ladder topology is the most widely used design for TFBAR filters as it has good power handling capabilities and also fewer resonators are required to achieve the desired filter performance [14]. Although the power handling capabilities are better for lattice-type filters, the numbers of resonators required are double than that for ladder configuration and implementation is also difficult [14].

The International Telecommunication Union has identified 2.6 GHz (2500−2690 MHz) as a global frequency band for international mobile telecommunications [15]. This band is suitable for applications which need higher

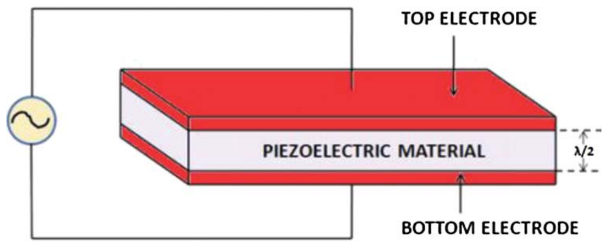

Figure 1: Schematic of TFBAR.

data rates from a large number of users like that in airports, urban areas, and other highly visited areas [15].

The article is presented in two sections. The first part presents the design and simulation of a TFBAR with zinc oxide (ZnO) as the piezoelectric layer and aluminium (Al) film as electrodes. In the second part, the modified Butterworth Van Dyke (MBVD) equivalent circuit is extracted from the simulation results and used in third- and fifth-order filter design. These filters are simulated in ladder topology using RF simulator. The filter parameters are obtained and compared.

2. TFBAR DESIGN AND SIMULATION

Finite element analysis based micro-electro-mechanical systems (MEMS) design tool Coventorware^{TM} is used for the design and simulation of the TFBAR. Silicon (Si) is used as a substrate material. It has low cost, is easily available, and is also mechanically robust which makes its handling easy during processing [12]. A 10 μm thick Si layer is supported by a 1 μm insulating layer of silicon oxide (SiO_2) layer on both front and back side. A thin zinc oxide is used as the piezoelectric film. It can be easily deposited by RF sputtering and has a relatively high coupling coefficient [12]. Aluminium (Al) film is used for top and bottom electrodes. Al has lower density and less mass loading than other metals like copper, silver, or gold, etc. which leads to higher resonant frequencies in TFBAR devices [1]. An air cavity is formed below the bottom electrode to confine the acoustic wave. The acoustic wave reflects between the top and bottom electrodes and a resonant mode is obtained.

To achieve a filter pass band, series and shunt TFBARs are arranged in a ladder formation. The shunt resonator has impedance versus frequency response which should be less than the series resonator. Because the resonators are to be fabricated on the same wafer, the thickness of the piezoelectric layer is fixed. Increasing the top electrode layer thickness, known as mass loading, is a practical process for altering the resonant frequency of the shunt resonator and producing the pass band when the

Table 1: Dimensions of different layers.

Resonator part	Material	Thickness (μm)	Area (μm^2)
Top electrode (series/shunt)	Aluminium film	0.20/0.25	200 × 200
Piezoelectric layer	Zinc oxide	1.0	350 × 350
Bottom electrode	Aluminium film	0.20	400 × 400

impedance of series resonators is low and impedance of the shunt resonator is high [16]. In the present design, the top electrode has a thickness of 0.20 μm for series resonator. To obtain an impedance response which is downshifted in frequency, the top electrode thickness is increased by 0.05 μm to 0.25 μm. The physical dimensions of different layers are mentioned in Table 1. Figure 2 shows a proposed process flow and the designed structure is shown in Figure 3.

Figure 4 shows the impedance versus frequency response of the series and shunt resonators; the effect of mass loading is evident in the graph whereby increasing thickness of the top electrode by 25%, the frequency is

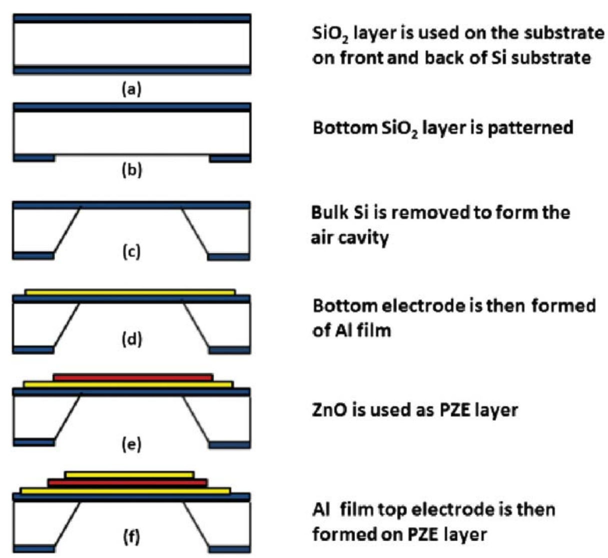

Figure 2: Proposed process flow.

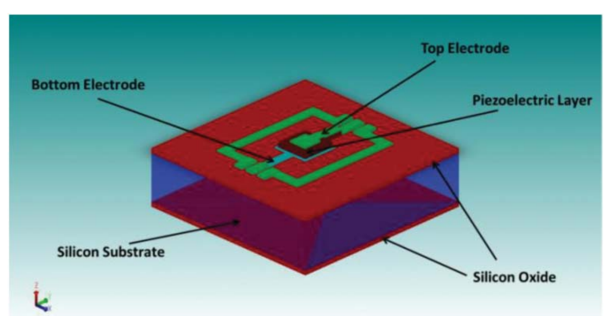

Figure 3: Designed TFBAR structure.

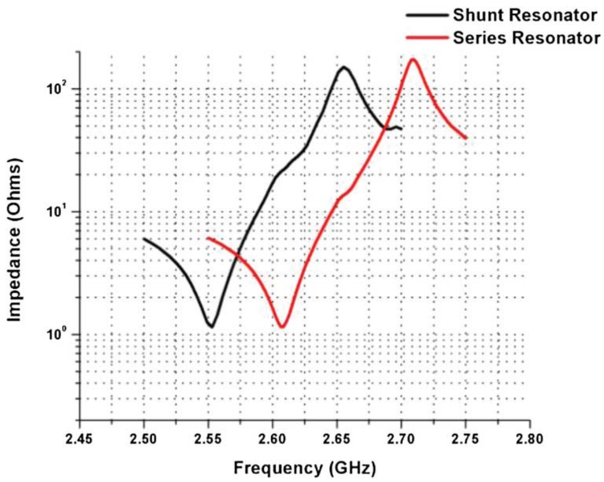

Figure 4: Impedance versus frequency response of the series and shunt resonators.

downshifted by around 2%. This downshifting of frequency is targeted to be around 1.5%–2% [12].

The DC analysis of the structure was done using MemMech solver with a 1 V DC potential applied to the top electrode. This analysis is done to compute the displacement of the piezo layer, charge, and static capacitance at the electrodes. The DC response yields a maximum displacement of 3.6 nm in the *z* direction for a voltage of 1 V as shown in Figure 5. A total charge of 4.19 pC is accumulated on each of the top and bottom piezo surfaces and the stack capacitance of the structure is 4.19 pF.

A modal analysis is then carried out to estimate the series and parallel breathing modes. The breathing modes occur when the top and bottom surfaces of the piezoelectric layer move in longitudinally opposite directions. The series resonance frequency is obtained with closed circuit conditions, i.e. where both electrodes are grounded and the resonance effect is derived from the structural effects only [17]. This is also known as mechanical resonance. The parallel resonant frequency is the frequency of the device when it is driven under constant charge conditions. To compute the parallel resonance frequency, the modal analysis of the structure is done with an open circuit condition where bottom electrode is grounded and the top electrode is left floating [17]. In addition, harmonic analysis is done to obtain the electrical impedance response and the quality factor (Q). Similar analysis is carried out for the shunt resonator also.

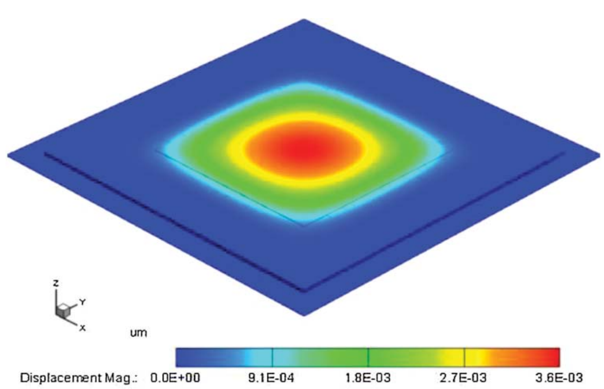

Figure 5: Displacement along *z* direction with a 1 V DC.

Table 2: **Summary of the TFBAR parameters**

Resonator	f_s (GHz)	f_p (GHz)	Q_s	Q_p	K^2_{eff}
Series	2.607	2.710	188.1	194.9	9.02%
Shunt	2.552	2.652	201.4	195.4	8.94%

3. FILTER DESIGN AND SIMULATION

For the series resonator, the series resonance frequncy f_s is 2.607 GHz and the parallel resonance frequncy f_p is 2.710 GHz. Q factor at series resonance frequency Q_s and the Q factor at parallel resonance frequency Q_p are 188.1 and 194.9, respectively. For the shunt resonator the series and parallel resonance frequencies f_s and f_p are 2.552 and 2.652 GHz, respectively. The Q factors at these frequencies, Q_s and Q_p, are 201.4 and 195.4, respectively. Table 2 summarizes these values along with the K^2_{eff} of the series and shunt resonators.

The MBVD equivalent circuits of both the resonators are extracted from these simulated results. The MBVD model was proposed in 1999 by Ruby et al. to improve the fitting accuracy between measured results and the BVD model [18]. The MBVD model, shown in Figure 6, consists of a first branch where L_m and C_m represent the acoustic (motional) behaviour of the resonator and R_m represents the mechanical losses. In the second parallel branch, C_0 is the electrostatic capacitance and R_0 is the electrical resistance. R_s is a series resistance that represents the losses due to electrodes. The expressions for these components are mentioned in Table 3, where ε_0 is the permittivity of free space and ε_r is the relative permittivity of the piezoelectric material. Q_s and Q_p are the series and parallel Q factors, respectively. f_s and f_p are the series and parallel

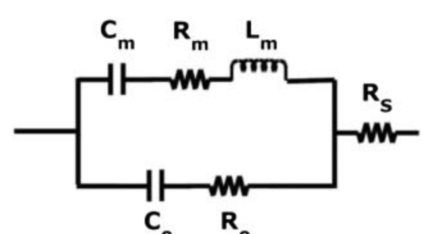

Figure 6: MBVD equivalent model of the TFBAR.

Table 3: Expressions for MBVD equivalent circuit [16]

$C_0 = \varepsilon_0\varepsilon_r\left(\frac{A}{d}\right)$	$C_m = C_0\left[\left(\frac{f_p}{f_s}\right)^2 - 1\right]$
$L_m = \frac{1}{C_m(2\pi f_s)^2}$	$R_m = \frac{2\pi L_m f_s}{Q_s}$
$R_o = \frac{1}{2\pi C_0 f_p Q_p}$	$R_s = \frac{R_\parallel L}{W}$

Table 4: Values for MBVD equivalent circuit

Component	C_o (pF)	L_m (nH)	C_m (pF)	R_m (ohms)	R_o (ohms)	R_s (ohms)
Series resonator	3.8	12.15	0.306	1.021	0.082	0.14
Shunt resonator	3.8	12.80	0.303	1.019	0.080	0.14

resonance frequencies, respectively. $R_\parallel$ is the square resistance of the electrodes, A is the electrode area, L and W are the length and width of the top electrode [16]. The values obtained for the components of the MBVD model are tabulated in Table 4.

Figure 7 shows the schematic diagram of a third- and a fifth-order filter. "1" represents the series resonator and "2" represents the shunt resonator. The size of the designed third-order and fifth-order filters are 1.0 mm × 1.20 mm and 1.50 mm × 1.80 mm, respectively. RF simulator is used to design and simulate the two filter configurations using the extracted values of MBVD model.

The return loss and insertion loss of the designed filters are shown in Figures 8 and 9. The third-order filter has an insertion loss of 1.62 dB and return loss of 18.97 dB with a bandwidth of 80 MHz whereas the fifth-order filter has an insertion loss of 2.85 dB, return loss of 25.28 dB, and a bandwidth of 60 MHz. These filter parameters are summarized in Table 5.

The insertion loss of the designed filters is high and it is expected to increase after fabrication. In [19], a 4 × 4

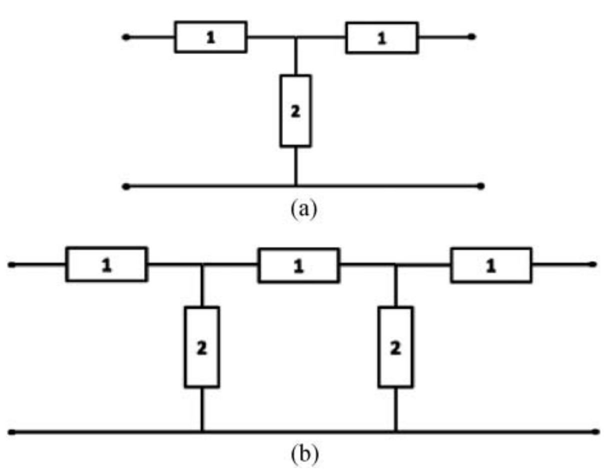

Figure 7: (a) Third-order filter and (b) fifth-order filter.

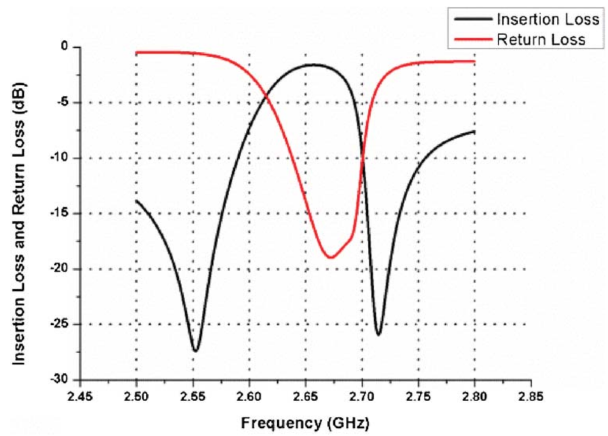

Figure 8: Response of third-order filter.

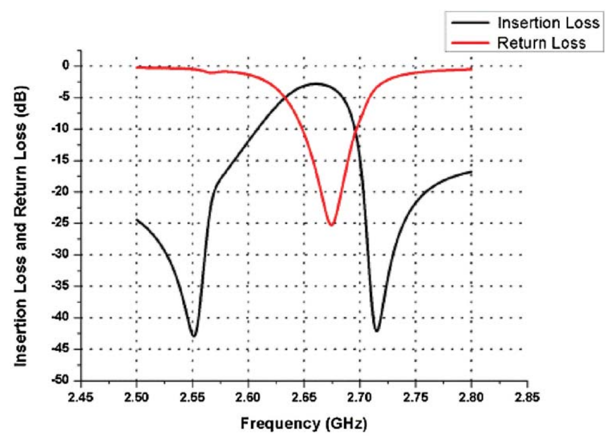

Figure 9: Response of fifth-order filter.

filter is designed with insertion loss of 3 dB which increases to around 5 dB after fabrication. This insertion loss is attributed to the fact that the anti-resonance frequency of the shunt resonator is not equal to the resonance frequency of the series resonator [19]. The minimum insertion loss of shunt resonator does not occur at the same frequency as the maximum value of the insertion loss for the series TFBAR. Therefore, signal power leaks through the shunt TFBAR, increasing the insertion loss. The anti-resonance frequency of the shunt resonator can be made equal to the resonance frequency of the series resonator by tuning the thickness of the shunt resonator [19]. Another way to decrease the insertion loss is by increasing the figure of merit (FOM) of the TFBAR, since insertion loss is inversely proportional

Table 5: Summary of filter characteristics

Parameter	Third-order	Fifth-order
Bandwidth	80 MHz	60 MHz
Insertion loss	1.62 dB	2.85 dB
Return loss	18.97 dB	25.28 dB

Table 6: **Comparison of insertion loss and return loss**

Reference	Frequency band	Insertion loss	Return loss
Present work	2.6 GHz band	1.62 dB	18.97 dB
Present work	2.6 GHz band	2.85 dB	25.28 dB
[20]	2.45 GHz	Within -3 dB* -10 dB#	<15 dB* <7 dB#
[21]	2010–2025 MHz	2 dB#	14 dB#
[22]	2 GHz	1.50 dB# (third-order) 2.36 dB# (fifth-order)	7–40 dB# (third-order) 11–30 dB# (fifth-order)
[23]	1.92–1.98 GHz	3.55 dB#	8.77 dB#
[24]	2.14 GHz	2.2 dB (min)* 2.9 dB (min)#	16.1 dB (max)* 12.7 dB (max)#

* simulated, # measured.

to the FOM for a resonator [12]. FOM for a TFBAR is the product of the coupling coefficient, K^2_{eff}, and the Q [12]. Since there is a design limitation on adjusting K^2_{eff}, therefore if Q is improved then the insertion loss could be reduced. Table 6 shows a comparison of the insertion loss and return loss of the designed filter with other reported work near the 2.6 GHz band.

4. CONCLUSION

TFBAR resonators have been designed for 2.6 GHz band frequency filter application. It is observed that as the filter order is increased from three to five, the bandwidth is reduced. The insertion losses of both the filters are high. The high insertion loss of the designed filter could be reduced by adjusting the thickness/structure of the shunt resonator or by increasing the FOM of the TFBAR. The fifth-order filter has a better performance in terms of the return loss by around 6 dB but the insertion loss gets degraded by around 1 dB. The designed filter could be used for RF filter applications in the 2.6 GHz band, specifically if insertion loss can further be reduced.

Acknowledgements

The authors wish to acknowledge Coventor Incorporation for their help and support.

ORCID

Jyotirmoy Dutta http://orcid.org/0000-0001-9347-144X
Atul Vir Singh http://orcid.org/0000-0001-9592-4406
Sonal Singhal http://orcid.org/0000-0002-5007-1718
Madhur Deo Upadhayay http://orcid.org/0000-0002-1246-2929

References

1. G. F. Perez-Sanchez, and A.-M. Acevedo, "Design of bulk acoustic wave resonators based on ZnO for filter applications," in *International Conference on Electrical Engineering, Computing Science and Automatic Control*, Toluca, 2009, pp. 1–6.
2. H. P. Loebl, C. Metzmacher, R. F. Milsom, P. Lok, F. Van Straten, and A. Tuinhout, "RF bulk acoustic wave resonators and filters," *J. Electroceram.*, Vol. 12, no. 1–2, pp. 109–18, Jan. 2004.
3. S. Jose, R. J. E. Hueting, and A. B. M. Jansman, "Modeling of bulk acoustic wave resonators for microwave filters," in *Proceedings of the 11th Annual Workshop on Semiconductor Advances for Future Electronics and Sensors*, Veldhoven, Netherlands, Nov. 27–28, 2008, pp. 558–61.
4. C. Vale, J. Rosenbaum, S. Horwitz, S. Krishnaswamy, and R. Moore., "FBAR filters at GHz frequencies," in *Proceedings of the 44th Annual Symposium on Frequency Control*, Baltimore, MD, May 23, 1990, pp. 332–6.
5. J. Y. Park, H. C. Lee, H. Kyeong Lee, J. Young Ko, and J. U. Bu, "Silicon bulk micromachined FBAR filters for W-CDMA applications," in *33rd European Microwave Conference*, Munich, Germany, 2003, pp. 907–10.
6. M. E. Hassan, E. Kerherve, Y. Deval, A. A. Shirakawa, P. Jarry, and A. Cathlin, "A study on FBAR filters reconfiguration," in *12th IEEE International Conference on Electronics, Circuits and Systems*, Gammarath, Tunisia, 2005, pp. 1–4.
7. M. El Hassan, E. Kerherve, Y. Deval, K. Baraka, J. B. David, and D. Belot, "Techniques for tuning BAW-SMR resonators for the 4th generation of mobile communications, modeling and measurement methods for acoustic waves and for acoustic microdevices," Available: http://www.intechopen.com/books/modeling-and-measurement-methods-for-acoustic-waves-and-for-acoustic-microdevices/techniques-for-tuning-baw-smr-resonators-for-the-4th-generation-of-mobile-communications
8. Z. Xinen, and A. Mortazawi, "Intrinsically switchable ferroelectric BAW resonators and filters," in *Proceedings of the 40th European Microwave Conference*, Paris, France, 2010, pp. 803–6.
9. S. Sis, V. Lee, and A. Mortazawi, " Intrinsically switchable, BST-on-silicon composite FBARs," in *IEEE MTT-S International Microwave Symposium Digest (MTT)*, Baltimore, MD, 2011, pp. 1–4.
10. V. Lee, A. S. Sis, S. Lee, and A. Mortazawi, "Intrinsically switchable ferroelectric bulk acoustic wave filters based on barium strontium titanate thin films," in *IEEE International Wireless Symposium (IWS)*, Beijing, China, 2013, pp. 1–4.
11. A. A. Sis, S. Ahmed, V. Lee, J. D. Phillips, and A. Mortazawi, "Intrinsically switchable thin film ferroelectric resonators," in *IEEE MTT-S International Microwave Symposium Digest (MTT)*, Montreal, Canada, 2012, pp. 1–3.
12. K.-y. Hashimoto, *RF Bulk Acoustic Wave Filters for Communications*. Artech House, Artech, Boston, 2009.
13. S. Rathod, A. Vir Singh, S. Chandra, and S. K. Kaul, "Design, fabrication and characterization of ZnO based thin film bulk acoustic resonators," *Adv. Mater. Res.*, Vol. 254, pp. 144–7, May 2011.
14. Y. Dae-Kim, K.-H. Sunwoo, S.-C. Sul, J.-H. Lee, D.-H. Kim, I.-S. Song, S.-H. Choa, and J.-G. Yook, "Highly miniaturized RF band pass filter based on thin-film bulk acoustic wave resonator for 5 GHz band application," *IEEE Trans. Microw. Theory Tech.*, Vol. 54, no. 3, pp. 1218–28, Mar. 2006.

15. “The 2.6 GHz spectrum band: An opportunity for global mobile,” Available: http://www.gsmworld.com/mobilebroadband
16. L. Catherinot, S. Giraud, M. Chatras, S. Bila, D. Cros, T. Baron, S. Ballandras, L. Estagerie, and P. Monfraix, “A general procedure for the design of bulk acoustic wave filters,” *Int. J. RF Microw. Comput. Aided Eng.*, Vol. 21, no. 5, pp. 458–65, Sep. 2011.
17. FBAR design tutorial, “‘MEMS design and analysis in analyzer’ Tutorials, Section-4 – ‘FBAR Analysis’, T4-1 to T4-38,” Coventorware, 2012.
18. H. Jin, S. R. Dong, J. K. Luo, and W. L. Milne, “Generalised Butterworth Van Dyke equivalent circuit for thin-film bilk acoustic resonator,” *Electron. Lett.*, Vol. 47, no. 7, pp. 424–6, Mar. 2011.
19. S. Qing-Xin, P. Kirby, E. Komuro, M. Imura, Q. Zghang, and R. Whatmore, “Thin film bulk acoustic resonators and filters using ZnO and lead-zirconium-titanate thin films,” *IEEE Trans. Microw. Theory Tech.*, Vol. 49, no. 4, pp. 769–78, Apr. 2001.
20. C. M. Fang, S. Pao, C. Lee, Y. Lu, P. Y. Chen, Y. C. Chin, and P. Z Chang, “Development of 2.4 GHz film bulk acoustic wave filter for wireless communication,” *J. Micro/Nanolithogr. MEMS MOEMS*, Vol. 8, no. 2, pp. 1–7, Apr. 2009.
21. H. Zhang, W. Pang, W. Chen, and C. Zhou, “Design of unbalanced and balanced radio frequency bulk acoustic wave filters for TD-SCDM,” in *International Conference on Microwave and Millimeter Wave Technology*, Chengudu, China, May 2010, pp. 878–81.
22. K. W. Kim, J. G. Yook, M. G. Gu, W. Y. Song, Y. J. Yoon, and H. K. Park, “TFBAR filters for 2 GHz wireless applications,” in *IEEE MTT-S International Microwave Symposium Digest*, Vol. 2, Seattle, WA, Jun. 2002, pp. 1181–4.
23. A. A. Shirakawa, P. Jarry, J. M. Pham, E. Korherve, F. Dumont, J.-S. David, and A. Cathelin, “Ladder-lattice bulk acoustic wave filters: Concept, design and implementation,” *Int. J. RF Microw. Comput. Aided Eng.*, Vol. 18, no. 5, pp. 476–84, Sep. 2008.
24. A. A. Shirakawa, M. El. Hassan, J.-M. Pham, P. Jarry, E. Kerherve, J.-B. David, F. Dumount, and D. Belot, “Method for improving ladder bulk acoustic wave filters rejection,” *Analog Integr. Circuits Signal Process.*, Vol. 55, pp. 69–75, Apr. 2008.

Authors

Jyotirmoy Dutta is a PhD research scholar in the Department of Electrical Engineering at the School of Engineering, Shiv Nadar University. He obtained his Master’s in electronics and communication engineering form NITTTR, Chandigarh. He is working in the area of RF MEMS, specifically, the design and simulation aspect of TFBAR based filters. He is a student member of the Institution of Electrical and Electronics Engineers (IEEE).

E-mail: jd222@snu.edu.in

Atul Vir Singh received his PhD from the Centre for Applied Research in Electronics, Indian Institute of Technology Delhi, New Delhi, in 2013. He is working in the area of MEMS technologies and has an extensive experience in MEMS processing techniques (surface and bulk micro-machining, anodic bonding, etch-stop, etc.) used to fabricate these devices. In order to promote MEMS research, he is developing a MEMS design and fabrication facility for the postgraduate and research students at the Shiv Nadar University.

E-mail: atul.singh@snu.edu.in

Sonal Singhal obtained her PhD from the Indian Institute of Technology Roorkee in 2011 during which she also availed Commonwealth Scholarship (Jan 2010 to Jan 2011) as split site scholar at Energy & Sustainable Research Division, University of Nottingham, UK. She has been working in the area of VLSI design and fabrication. Her research interests include topics like design of novel semiconductor, electronic and optoelectronic devices, very large scale integration (VLSI) technology and design, network realization in HDL. She is also a recipient of an externally funded project under the Fast Track Young Scientist Scheme, DST, India (2012) on the fabrication of photo voltaic (PV) devices.

E-mail: sonal.singhal@snu.edu.in

Madhur Deo Upadhayay received Master of Engineering in microwave communication and radar engineering and Bachelor of Engineering in electronics and communication engineering from Dr. Bhimrao Ambedkar University Agra, India, in 2004 and 2002, and PhD degree in microwave and RF engineering from the Indian Institute of Technology, Delhi, India, in 2014., He is an assistant professor in the Department of Electrical Engineering, Shiv Nadar University, India, where he is involved in teaching and research activities. His research interest includes: microwave integrated circuits (active, passive, reconfigurable), RF MEMS, reconfigurable/active antennas. He is a member of the IEEE, USA, and associate member of the Institution of Electronics and Telecommunication Engineers (IETE) India.

E-mail: madhur.upadhayay@snu.edu.in